Vacuum Sol-Gel Synthesis and Characterization of $NiAl_2O_4$ Nanoparticles

N. N. Zurita-Méndez[a], M.A. Espinosa-Medina[a], G. Carbajal-De la Torre[a]*

[a] Facultad de Ingeniería Mecánica, Universidad Michoacana de San Nicolás de Hidalgo, C.P. 58000; Morelia, Michoacán, México.

* Corresponding author, E-mail: georginacar@gmail.com

Received: 03-11-2020 Accepted: 02-08-2021
Published: 17-09-2021

ABSTRACT

Nowadays, there is a big interest in the preparation of mixed oxides with transition metal atoms. Spinel oxides of AB_2O_4 formula present structural properties that make them attractive in magnetic applications, sensor technology and refractory materials [1]. The nickel aluminate structure $NiAl_2O_4$, makes it resistant to acids and alkalis, presents high melting point and surface area, extraordinary catalytic properties and is resistant to deactivation by coke formation [2]. Those properties allow a wide use in the oil industry in processes as hydrogenation, methanation and steam reforming [3, 4]; this material is also employed in high temperature fuel cells and as an anode for the production of aluminum [5]. In this work, we report the production of nickel aluminate nanoparticles ($NiAl_2O_4$) with a considerable magnetic field of 137.09 Oe by employing a -300 Hg mm vacuum sol-gel chemical synthesis. The material was evaluated through Differential Scanning Calorimetry, Thermogravimetric analysis (DSC/TGA), Fourier Transform Infrared spectroscopy (FTIR), X-Ray Diffraction analysis (XRD), Scanning Electron Microscopy (SEM), high resolution Transmission Electron Microscopy (HR-TEM) analysis and its magnetic behavior was corroborated by a vibrating sample magnetometer (VSM). Preliminary results show the formation of $NiAl_2O_4$ nanocrystals with dimension of 5 to 15 nanometers, homogeneous morphology, inverse spinel structure and weak ferromagnetic behavior with a coercive field (H_c) of 66.29 Oe, a remainder magnetization (M_r) of 7.15 emu/g and a saturation magnetization (M_s) of 71.34 emu/g.

Keywords: Sol-gel synthesis; spinel structure; nanocrystals; coercivity.

Síntesis por sol-gel a vacío y caracterización de nanopartículas de $NiAl_2O_4$

RESUMEN

Actualmente, existe un gran interés en la obtención de óxidos mixtos con átomos de metales de transición. Los óxidos de espinela de fórmula AB_2O_4 presentan propiedades estructurales que los hacen atractivos en aplicaciones magnéticas, de tecnología de sensores y como materiales refractarios [1]. La estructura del aluminato de níquel $NiAl_2O_4$, hace esta espinela resistente a ácidos y álcalis, con un alto punto de fusión y elevada área superficial, extraordinarias propiedades catalíticas y resistencia a la desactivación por formación de coque [2], esas propiedades permiten un amplio uso en la industria petrolera en procesos como hidrogenación, metanización y reformado con vapor [3,4]; Este material también se emplea en celdas de combustible de alta temperatura y como un ánodo para la producción de aluminio [5]. En este trabajo, se desarrolló la producción de nanopartículas de aluminato de níquel ($NiAl_2O_4$) con un campo magnético de 137.09 Oe mediante síntesis química por sol-gel con un vacío de -300 Hg mm. El material se evaluó mediante Calorimetría Diferencial de barrido, Análisis Termogravimétrico (DSC / TGA), Espectroscopía Infrarroja por Transformada de Fourier (FTIR), análisis de Difracción de Rayos X (XRD), Microscopía Electrónica de Barrido (SEM), Microscopía Electrónica de Transmisión de alta resolución (HR-TEM) y su comportamiento magnético fue corroborado con un magnetómetro de muestra vibrante (VSM). Los resultados preliminares muestran la formación de nanocristales de $NiAl_2O_4$ con una dimensión de 5 a 15 nanómetros, morfología homogénea, estructura de espinela inversa y comportamiento ferromagnético débil con un campo coercitivo (Hc) de 66.29 Oe, una magnetización remanente (Mr) de 7.15 emu / g y una magnetización de saturación (Ms) de 71.34 emu / g.

Palabras claves: Síntesis sol-gel, estructura espinela, nanocristales, coercividad.

INTRODUCTION

The group of A_2BX_4 materials with A and B elements and X a chalcogen (O, S, Se, Te), has attracted much attention since it offers a versatile range of relevant physical and chemical properties [6,7]. The nickel aluminate $NiAl_2O_4$ is an inverse spinel, in which, half of the aluminum ions

preferentially fill the tetrahedral sites and the other ones occupies the octahedral sites. Mixed metal oxide spinels as $NiAl_2O_4$ are worth studied due to the large surface area and high stability [8], and it is one of the most important aluminates especially for it use as catalyst, pigment and magnetic material. It has been reported that in general, smaller particle size has beneficial higher specific surface area for catalytic applications of the $NiAl_2O_4$ [9] so that synthesis of nanosized nickel aluminate particles is of great interest for the previous applications. Among the processes for the obtainment the spinel oxides, the sol-gel method is described [10, 11], it represents an option to produce pure and nanometric powders by the generation of an organometallic solution (sol) which is composed of chains of metal ions and oxygens to subsequently produce a rigid gel. This method has several advantages as economy, low temperatures operation, distribution of phases in multicomponent systems, among others. Nevertheless, the sol-gel synthesis developed involves the inclusion of controlling the atmosphere with vacuum at -300 mm Hg. The modification of this factor makes it possible to produce oxides systems with micro and nanostructures potentially optimized that favors improvement in their catalytic performance as described ahead.

MATERIAL AND METHODS

The preparation of the $NiAl_2O_4$ nanoparticles was carried out with a sol-gel methodology, and in order to control the oxidation of the precursors and the homogeneity of the product, a vacuum of -300 Hg mm was applied. The precursors employed were aluminum isopropoxide [$Al(OC_3H_7)_3$], nickel (II) chloride ($NiCl_2$) and 1-propanol (C_3H_7OH) as solvent; all of them in reactive grade quality. The reaction last 72 hours at 80°C with constant agitation (figure 1). Subsequently, the obtained sol was dried at 60°C during 48 hours, and then, after the DSC/TGA evaluations, the material was sintered at 600°C, 800°C, and 1100°C due to its thermal behavior which is explained in the results and discussion section.

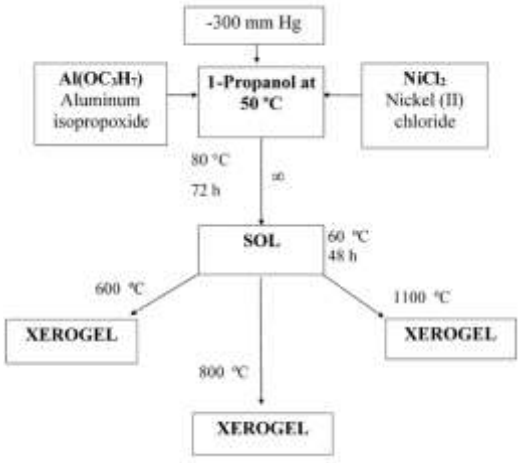

Fig. 1. The experimental sol-gel method diagram employed.

The obtained samples were characterized with a NETZCH STA 449F3 calorimeter in an 80/20 nitrogen/air atmosphere between a temperature range of 100°C to 1000°C and a heating rate of 10°C min^{-1}. The subsequent sintering was carried out in a conventional FELISA furnace under atmospheric conditions for four hours each.

The identification of the product obtained by X-ray diffraction (XRD) was carried out in a D8 Advanced Da Vinci diffractometer with CuKα radiation at an angle of 2θ, in a range of 20º - 90º and a rate of 0.04º min^{-1}. The identified phases were indexed for the adjustment of the sample profile with the software integrated to the diffractometer. The morphological and nanostructure analysis by Scanning Electron Microscopy (SEM) was performed in a high resolution (1 nm) microscope JeolJSM 7600F, equipped with a Bruker dispersive energy spectrometer (EDS). The particle size was determined by the use of the Scherrer formula (1). The surface area analysis was obtained by nitrogen absorption with the Brunauer Emmet Teller (BET) isotherm equation Quantachrome, model Quantasorb Jr, for powders and small monoliths and the magnetic behavior obtained through a SQUID vibrating sample magnetometer (VSM) Quantum Design, showed the formation of $NiAl_2O_4$ nanoparticles with weak ferromagnetic behavior, when they were sintered at 1100°C. The magnetic properties of

the $NiAl_2O_4$ powders were measured at room temperature with an applied field from -15000 Oe to +15000 Oe in a SQUID vibrating sample magnetometer (VSM) Quantum Design, this interval was chosen according to several studies, where similar materials were also evaluated by this technique [12, 13]

RESULTS AND DISCUSSION

To stablish the relationship of the $NiAl_2O_4$ powders and their changes with temperature and time, thermogravimetric analysis (TGA) and Differential Scanning Calorimetry (DSC) were performed. The loss of mass shown in the thermogram in figure 2 coincided with that expected for solvent (1-propanol) and to the decomposition chemical reactions for the initial formed salts, the loss of mass continues to the 750°C, which means that a thermal treatment at 800°C must be realized. The DSC analysis shows endothermic peaks at 172°C, 588°C and 757°C attributed to the solvent evaporation which is adsorbed physically into the porous of the material. About 500°C and 670°C, two exothermic peaks appear, and they can be caused to the combustion of the alcoxide group which remains attached to the $NiAl_2O_4$ structure. The first stage of the thermogram (100°C – 400°C) represents the solvent removal and adsorbed species, while the second stage (450°C – 1000°C) suggest the initial salts decomposition in nickel oxides and nickel aluminates [14, 15]. FTIR is an invaluable tool for analyzing the structure of the $NiAl_2O_4$ powders, because the frequencies at which the IR radiation is absorbed forms peaks that can be directly correlated to bonds within the synthetized compound. When the material formed is irradiated, the radiation usually excites molecules into a higher vibrational state, making it possible to observe the wavelength of light absorbed as a function of the energy difference between the "at-rest" and "excited" vibrational states. The obtained FTIR spectrum (see figure 3) shows peaks near 300 - 900 cm^{-1}, which are characteristic vibrational peaks of the spinel phase and are associated to the Ni-O-Al bonds [16].

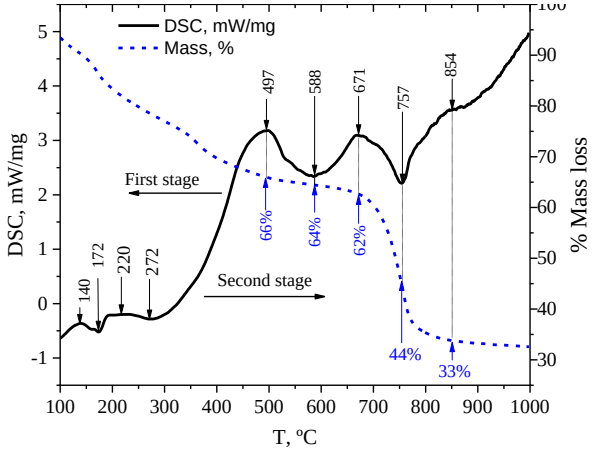

Fig. 2. TGA-DSC curves of powders containing $NiO/NiAl_2O_4$ obtained through the sol-gel method.

The -OH bonds in an alcohol absorption were near the 1350 - 14700 cm^{-1} wavelength representing the presence of the solvent (1-propanol) as the observed broad peak at 3100 - 3500 cm^{-1} is possibly assigned to the surface adsorbed solvent. Bands at 1350 - 1470 cm^{-1} could be due to the CH_3 and CH_2 deformation vibration of the precursor alkoxide groups, suggesting that some of the propoxide molecules were still attached to the NiO and $NiAl_2O_4$ products.

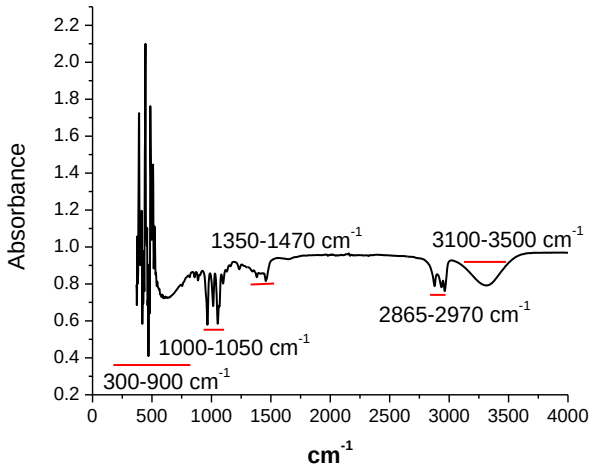

Fig. 3. FTIR spectrum of the NiO-$NiAl_2O_4$ powders.

Once the TGA-DSC diagram was analyzed and interpreted, the magnetic NiO-$NiAl_2O_4$ powders were thermally treated at 600ºC, 800°C and 1100ºC in a conventional furnace for 4 hours and pulverized in a ceramic mortar. To identify the phases of the materials, they were examined through the XRD technique. Figure 4 shows the X-ray diffraction, in

which the patterns of the peaks act as a unique fingerprint of the crystallographic unit cell within a crystalline substance. They can be identified by comparing measured peak positions with the database. The peaks in 2θ = 19.10, 31.44, 37.05, 45.06, 55.98, 59.71, 65.63, 77.83 and 83.17 of the crystallographic base COD: 9005989, fit adequately with the spinel cubic structure reflections (space group Fd3m) of the nickel aluminate $NiAl_2O_4$ with Miller indices denoted by [1,1,1]; [2,2,0]; [3,1,1]; [4,0,0]; [4,2,2]; [3,3,3], [4,4,0]; [5,3,3] and [4,4,4]; for each peak. When the sample was sintered at 600°C, the NiO phase is the most observable, this is due to the amorphous phase of the aluminate and the small size of grains, this behavior strengthens the hypothesis that generally at high temperatures the nucleation rate is lower, which increases the size of the particle nucleus [17].

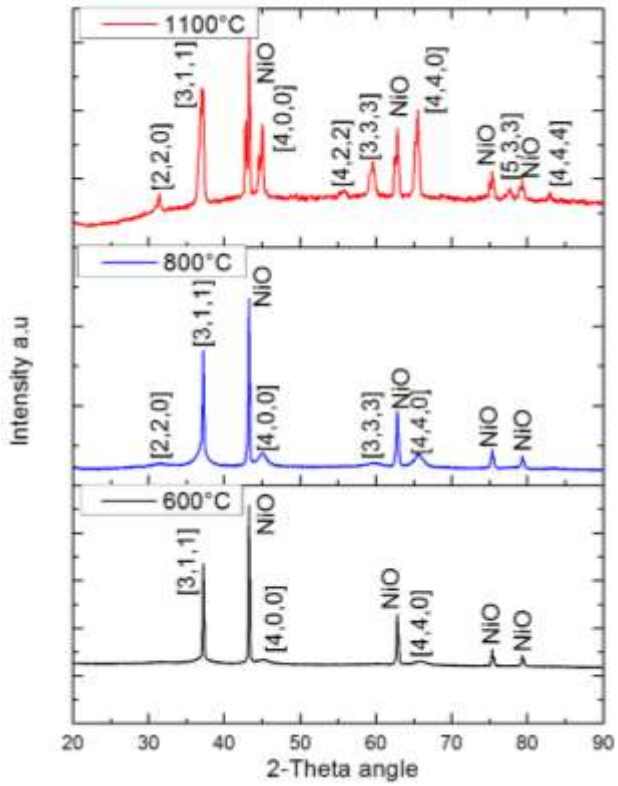

Fig. 4. The XRD pattern of the NiO-$NiAl_2O_4$ prepared through the vacuum sol-gel method and sintered at 600ºC, 800°C and 1100°C.

According to the indexed XRD pattern which matches to the synthetized sample, it is possible to identify the spinel structure of the oxide obtained and whose atomic arrangement is illustrated in figure 5. It can be analyzed that half of the aluminum ions preferentially fill the tetrahedral sites while the other half occupies the octahedral sites. Under this study is that the compound obtained can be represented by the formula $(Al^{3+})_A[Ni^{2+}Al^{3+}]_BO_4^{2-}$, where A and B represent the tetrahedral and octahedral sites respectively [18].

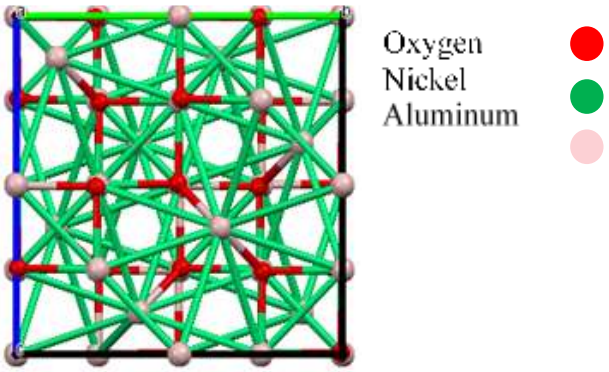

Fig. 5. Unit cell for the spinel arrangement obtainment $NiAl_2O_4$

The particle size (Dp) was calculated using the Scherrer equation (1):

$$D_p = \frac{B\lambda}{\beta Cos\theta} \qquad (1)$$

Where *Dp* is the average particle size, *B* is the Scherrer constant (0.94), β the amplitude of the peak in radians, θ is the Bragg angle and λ is the wavelength of the incident ray (0.154 nm). The full width at half maximum value (FWHM) of each diffraction peak was measured with the Origin 8.6 software, and they are expressed in table 1, for the samples sintered at 600°C, 800°C, and 1100°C respectively. The calculated average particle size of the nickel aluminate crystals is about 5.02 nm for the phase sintered at 600°C, 10.71 nm for the material taken to 800°C and 14.53 nm for the particles with thermal treatment at 1100°C.

The Scanning Electron Microscopy analysis shows high resolution images of the powders obtained. The

morphology of the nickel aluminate when sintered at 600°C as well as the particle homogeneity are shown in figure 6. It can be observed a strong agglomeration of particles due to the Van Der Waal forces. Subsequently, by increasing the sintered temperature at 800°C and 1100°C, it is found that the acquired morphology begins to be more crystalline as the XRD analysis showed for the nickel aluminate phase (figure 4). A semispherical morphology for nickel aluminate particles can be observed when sintered at 800°C; however, the agglomeration of particles continues as shown in figures 7 and 8. In figure 8b, the nanometric size of the nickel aluminate particles can be detailed. The general EDS analysis is shown in table 2. The images of the sample sintered at 1100°C obtained by TEM are given in figure 9. The particle sizes calculated by XRD analysis were in accordance with TEM images, where the nanoparticles present agglomerations, which, in addition to the Van Der Waals forces, present magnetic properties as indicated by the hysteresis loop obtained by VSM analysis (figure 9a to 9c). A soft magnetic material has a small quantity of remaining magnetization after switching off the magnetic field, thus presenting a slender hysteresis curve and consequently small coercivity and remanence values. Soft magnetic materials are used in devices in which a change in magnetization during the operation is desirable. They show small coercive fields in the range of -100 Oe, and therefore less magnetic field is required to reach zero magnetization [19].

Table 1. Calculation of the average particle size by using the Scherrer equation (1) for each thermal treatment carried out in the synthesis of nickel aluminate $NiAl_2O_4$.

ANGLE (2Θ)	**[1] *hkl***	**TEMPERATURE:**					
		600°C		**800°C**		**1100°C**	
		FWHM	**[2] *PS***	**FWHM**	**[2] *PS***	**FWHM**	**[2] *PS***
31.44	[2,2,0]					0.5317	16.22
37.05	[3,1,1]	0.7360	11.89	0.6793	12.89	0.7454	11.75
45.06	[4,0,0]	3.1036	2.90	2.6651	3.37	3.1447	2.86
55.98	[4,2,2]					29.385	0.32
59.71	[3,3,3]			0.84	11.39	0.6671	14.35
65.63	[4,4,0]	36.7707	0.27	0.65	15.20	0.6126	16.12
77.83	[5,3,3]					17.194	0.62
83.17	[4,4,4]					0.2054	54.04
AVERAGE PARTICLE SIZE			**5.02**		**10.71**		**14.53**

[1] *hkl*: miller indices, **[2] *PS***: particle size (nm)

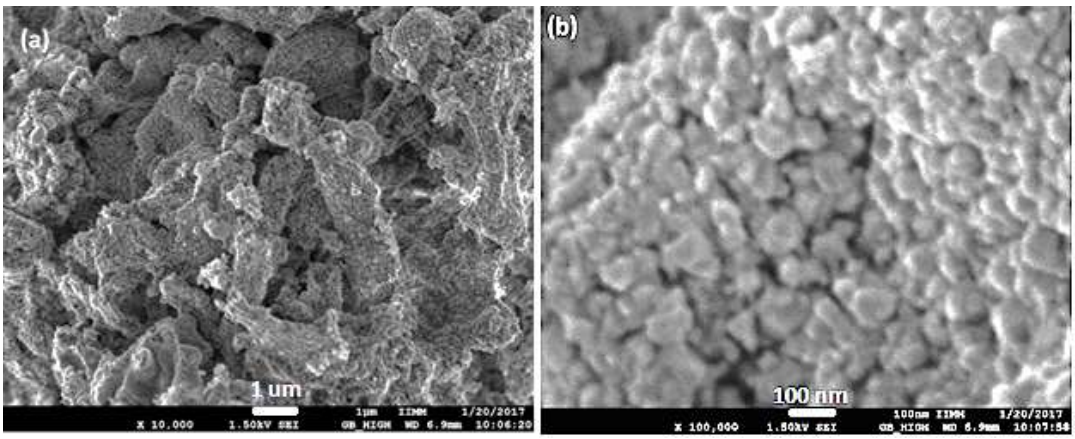

Fig. 6. SEM image for the obtained sample containing $NiAl_2O_4$, when sintered at 600°C: a) Close up to X 10,000 and b) Close up to X 100,000.

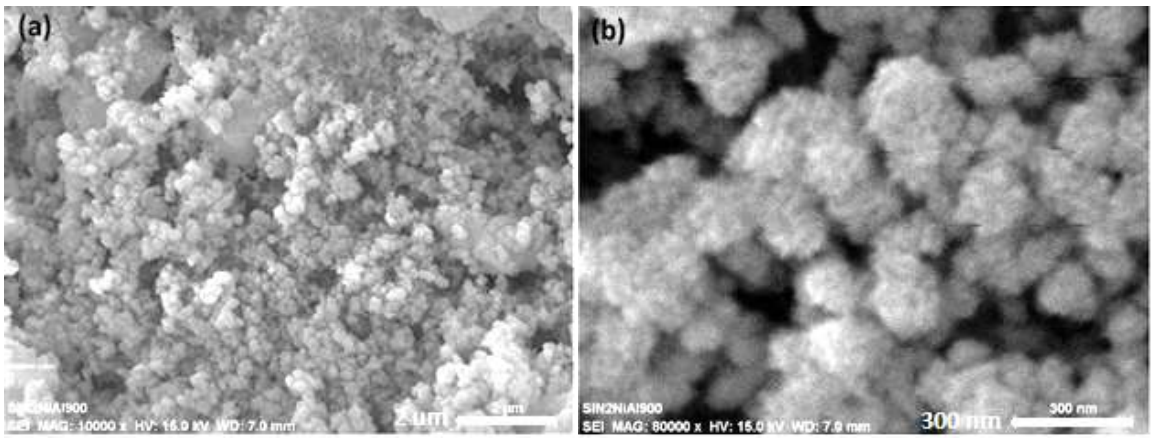

Fig. 7. SEM image for the obtained sample containing $NiAl_2O_4$, sintered at 800°C: a) X 10,000 and b) X 80,000.

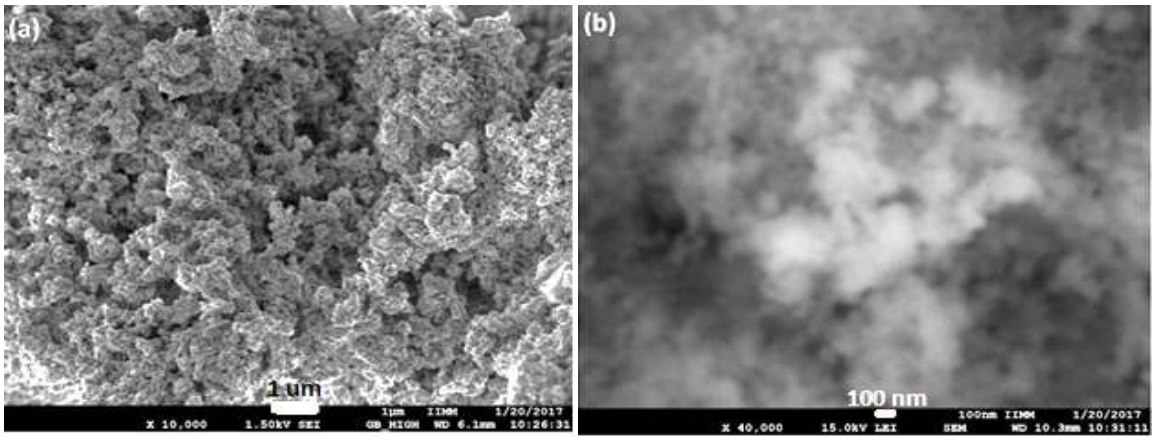

Fig. 8. Morphology and particle size for the obtained sample containing $NiAl_2O_4$, when sintered at 1100°C: a) Close up to X 10,000 and b) Close up to X 40,000 X.

Table 2. General EDS analysis for the obtained samples containing $NiAl_2O_4$, when sintered at 600°C, 800°C and 1100°C.

ELEMENT	**ATOMIC %**		
	600°C	800°C	1100°C
O	36.89	42.46	52.35
Al	25.14	24.03	21.40
Ni	37.97	33.52	26.25

Figure 10 shows the VSM plot of the nickel aluminate $NiAl_2O_4$ powders. The ferromagnetic behavior of the binary mixed oxide calcined at 1100°C presented a very narrow hysteresis loop with a very low coercive field (Hc=66.29 Oe). The retentivity (Mr) was read at 7.15 emu/g with a magnetic saturation (Ms) of 71.34 emu/g, representing high magnetic permeability and high flux density at saturation [20].

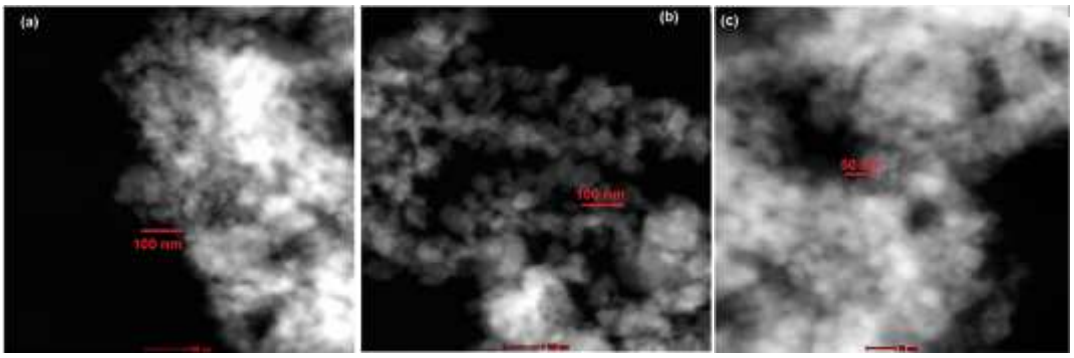

Fig. 9. a), b) and c) TEM images of vacuum sol-gel samples sintered at 1100°C.

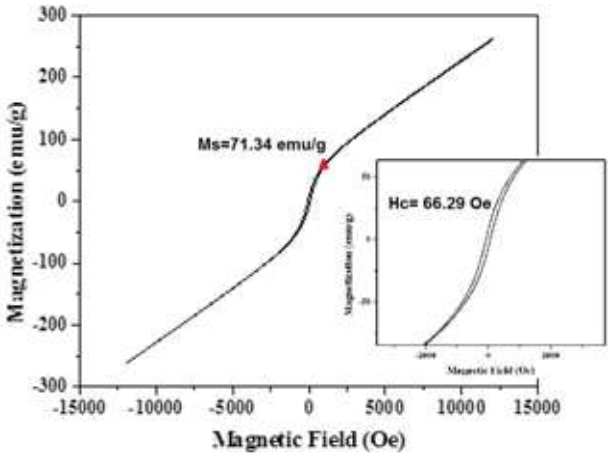

Fig. 10. The hysteresis loop of $NiAl_2O_4$ in a M-H representation.

Subsequently, the samples were taken to a cryogenic storage Dewar with liquid nitrogen, all the air was evacuated from the glass cell and small amounts of the adsorbate were added. The results of the surface area for the samples analyzed are shown in table 3, it can be observed that the temperature effect when it is incremented, decreases the surface area and increase the crystal distance.

Table 3. Surface area determined by BET for the samples containing $NiAl_2O_4$, when sintered at 800 °C and 1100 °C.

Sample	Surface area BET (m^2/g)
$NiAl_2O_4$ (800°C)	87.98
$NiAl_2O_4$ (1100°C)	68.19

As the particle size decreases, it is expected that the surface area per mass unit increases. For a catalyst material, this value is related to its activity, this is due to the fact that heterogeneous catalysis usually takes place by sequences of reactions involving fluid-phase reagents and the exposed layer of the solid catalyst surface, the estimation of the surface area of the material, and its general catalytic activity are initially based on the morphology. Besides influencing the structure of nanomaterials, temperature also contributes to the shape and purity of materials as observed in this investigation where the values obtained agree with the concept of the particle size ratio, the sintering temperature and the surface area.

CONCLUSIONS

$NiAl_2O_4$ nickel aluminate nanoparticles with spine structure and magnetic behavior of sizes between 5 and 15 nm were obtained with a -300 Hg mm vacuum sol-gel methodology. Due to the interaction of Van Der Waal forces in the nanoparticles, they showed agglomerations, so it is necessary to apply a dispersant that promotes sufficient stabilization that allows the development of a high-performance catalyst. The sintering temperature plays an important role in the surface area of the spinel, that is a reason for which it is necessary to perform a detailed analysis to find the temperature to optimize the compound obtained. The catalyst obtained presents a ferromagnetic behavior with a very low coercive field (Hc = 66.29 Oe). The retentivity (Mr) was read at 7.15 emu/g with a magnetic saturation (Ms) of 71.34 emu/g, representing high magnetic permeability and high flux density at saturation. As described in this investigation, the controlled vacuum in which the sol-gel synthesis was developed, allowed to

obtain $NiAl_2O_4$ nanoparticles, with high purity and promissory uses as catalyst.

ACKNOWLEDGEMENTS

Authors acknowledge the given support of the Material Degradation Laboratory from Mechanical Engineering Faculty (UMSNH) for the research development. The present research was supported by the research project number 243236 of CB-2014-02 from the I0017 fund of the CONACYT.

REFERENCES

[1] Ragupathi C., Vijaya J.J., Surendhar P., Kennedy L.J. (2014) "Comparative investigation of nickel aluminate (NiAl2O4) nano and microstructures for the structural, optical and catalytic properties" *Polyhedron* 72:1-7.

[2] Utchariyajit K., Gulari E., Wongkasemjit S. (2006) "The use of alumatrane for the preparation of high-surface-area nickel aluminate and its activity for CO oxidation" *Appl. Organomet. Chem.* 20(1):81-88.

[3] Ragupathi C., Vijaya J.J., Kennedy L.J. (2014) "Preparation, characterization and catalytic properties of nickel aluminate nanoparticles: A comparison between conventional and microwave method" *J. Saudi Chem. Soc.* 21:S231-S239.

[4] Rodríguez J.C., Marchi A.J., Borgna A., Monzón A. (1997) "Effect of Zn Content on Catalytic Activity and Physicochemical Properties of Ni-Based Catalysts for Selective Hydrogenation of Acetylene" *J. Catal*. 171(1):268-278.

[5] Nazemi M.K., Sheibani S., Rashchi F., Gonzalez de la Cruz V.M., Caballero A. (2012) "Preparation of nanostructured nickel aluminate spinel powder from spent NiO/Al_2O_3 catalyst by mechano-chemical synthesis" *Adv. Powder Technol.* 23(6):833-838.

[6] Zhang X., Stevanović V., D'Avezac M., Lany S., Zunger A. (2012) "Prediction of A2BX4 metal-chalcogenide compounds via first-principles thermodynamics" *Phys. Rev. B: Condens. Matter.* 86(1):014109.

[7] Abaide E.R., Anchieta C.G., Foletto V.S., Reinehr B., Nunes L.F., Kuhn R.C., Mazutti M.A., Foletto E.L. (2015) "Production of copper and cobalt aluminate spinels and their application as supports for inulinase immobilization" *Mater. Res.* 18(5):1062-1069.

[8] Salleh N.F.M., Jalil A.A., Triwahyono S., Efendi J., Mukti R.R., Hameed B.H. (2015) "New insight into electrochemical-induced synthesis of NiAl2O4/Al2O3: Synergistic effect of surface hydroxyl groups and magnetism for enhanced adsorptivity of Pd(II)" *Appl. Surf. Sci.* 349:485-495.

[9] Chan Y.-T., Wu C.-H., Shen P., and Chen S.-Y. (2014) "Nickel aluminate oxides/hydroxides by pulsed laser ablation of $NiAl_2O_4$ powder in water" *Appl. Phys. A* 116(3):1065-1073.

[10] Sajjadia S.M., Haghighia M., Rahmania F. (2015) "Syngas production from CO_2-reforming of CH_4 over Sol-Gel synthesized $Ni\text{-}Co/Al_2O_3\text{-}MgO\text{-}ZrO_2$ Nanocatalyst: Effect of ZrO_2 precursor on catalyst properties and performance" *Quim. Nova* 38(4):459-465.

[11] Alvarado Navarro J., Aguilar Gabid J.A. (2006) "Comparación entre $MgAl_2O_4$ sintetizado por medio de sol-gel contra otros métodos" *Ingenierías* 9(31):45-51.

[12] Ban I., Stergar J., Drofenik M., Ferk G., Makovec D. (2011) "Synthesis of copper–nickel nanoparticles prepared by mechanical milling for use in magnetic hyperthermia" *J. Magn. Magn. Mater.* 323(17):2254-2258.

[13] Ragupathi C., Vijaya J.J., Kennedy L.J., Bououdina M. (2014) "Combustion synthesis, structure, magnetic and optical properties of cobalt aluminate spinel nanocrystals" *Ceram. Int.* 40(8):13067-13074.

[14] Zurita-Méndez N.N., Carbajal-De la Torre G., Cadenas E., Liu H., Espinosa-Medina M.A. (2018) "Synthesis and characterization of nickel aluminate nanoparticles" *Mater. Res. Express* 6.

[15] Nazemi M.K., Sheibani S., Rashchi F., Gonzalez de la Cruz V.M., Caballero A. (2012) "Preparation of nanostructured nickel aluminate spinel powder from spent NiO/Al2O3 catalyst by mechano-chemical synthesis" *Adv. Powder Technol.* 23(6):833-838.

[16] Anchieta C.G., Tochetto L., Madalosso H.B., Sulkovski R.D., Serpa C., Mazutti M.A., De Almeida A., Gündel A., Foletto E.L. (2015) "Effect of thermal treatment on the synthesis of $NiAl_2O_4$ spinel oxide using chitosan as precursor" *Cerâmica* 61(360):477-481.

[17] Carbone M. (2016) "Cu-Zn-Co nanosized mixed oxides prepared from hydroxycarbonate precursors" *J. Alloys Compd.* 688:202-209.

[18] Deraz N.M. (2013) "Synthesis and Characterization of Nano-Sized Nickel Aluminate Spinel Crystals" *Int. J. Electrochem. Sci.* 8:5203-5212.

[19] Hedayatnasab Z., Abnisa F., Daud W.M.A.W. (2017) "Review on magnetic nanoparticles for magnetic nanofluid hyperthermia application" *Mater. Des.*, 123:174-196.

[20] Gavrila H., Ionita V. (2002) "Crystalline and amorphous soft magnetic materials and their applications- status of art and challenges" *J. Optoelectron. Adv. Mater*. 4(2):173-191.